Wireless Netw (2018) 24:2409–2426
https://doi.org/10.1007/s11276-017-1479-0

Moving network based on mmWave technology: a promising solution for 5G vehicular users

Antonio Mastrosimone[1] · **Daniela Panno**[1]

Published online: 3 March 2017

Abstract Mobile connectivity is a vital requirement for people's everyday life. Users would like to have unlimited access to information for anyone, anywhere, and anytime, especially in public means of transport where they spend a lot of time travelling. The connectivity to Internet becomes difficult for passengers because public transportation vehicles suffer from the low quality signal from the outside wireless network. A first solution to improve the broadband connectivity is to deploy more eNodeBs close to busses or train routes, but it requires high investment for providers and a higher complexity in managing the increasing number of handover. The rapid growth in the deployment of LTE femtocells for indoor use and their benefits have led many authors to propose using them even in vehicles, implementing the so-called Moving Networks. This paper shows that the use of pure LTE mobile femtocells exhibits relevant issues in terms of interference and consequently poor performance in a realistic use. In order to overcome these issues, we propose to adopt the millimeter Wave (mmWave) technology in the Moving Networks, creating the Hybrid Mobile Femtocells. In the paper we discuss the concerns arising from applying mmWave communications at 60 GHz inside vehicles. We provide a new throughput analysis in order to benchmark our proposal to the solutions presented in literature. Furthermore, we analyse the system performance in two different scenarios: a sub-urban setup and in an urban configuration where different kind of cells are deployed. The results obtained by Matlab simulations, show a noticeable improvement of the global system throughput by using Hybrid Mobile Femtocells.

Keywords Moving Networks · LTE · Millimeter-Waves · Mobile Femtocells · 60 GHz · Hybrid Mobile Femtocells

Abbreviations

$SINR_y^x$	Signal to interference plus noise ratio measured in the link $\boldsymbol{y}$ (y ∈ [D, A, B]) using the solution $\boldsymbol{x}$ (x ∈ [W, N, O, H])
Th^x	Throughput of the Moving Network solution x (x ∈ [W, N, O, H])
L_{zz} (d)	Propagation model in the link zz at the distance d
$S(\sigma_i)$	Log-normal shadowing effect considering a standard deviation σ_i
D	Direct link
A	Access link
B	Backhaul link
W	Moving Network solution without MFAP
O	Moving Network solution with L-MFAP that operates in orthogonal allocation scheme
N	Moving Network solution with L-MFAP that operates in non-orthogonal allocation scheme
H	Moving Network Solution with H-MFAP
I_f	Interference contribution due to the neighboring L-MFAPs
I_M	Interference contribution due to the neighboring eNodeB
I_{MFAP}	Interference contribution of the nearby MFAP
I_p	Interference contribution of the nearby picocells
N_{RB}	Number of LTE resource block
N_{UE}	Total number of user equipment

✉ Antonio Mastrosimone
antonio.mastrosimone@dieei.unict.it

Daniela Panno
daniela.panno@dieei.unict.it

[1] Department of Electrical, Electronics and Computer Engineering, University of Catania, Catania, Italy

N_{VUE}	Number of vehicular user equipment
N_{out_UE}	Number of outside user equipment
N	Number of pico_UEs
$N_{VUE,j}$	Number of VUEs inside the MFAP j
$Th^{x}_{VUE,jk}$	Throughput of the *k*th VUE inside the MFAP j, using the solution *x*
$Th^{x}_{out\_UE,i}$	Throughput of the *i*th out_UE using the solution *x*

1 Introduction

Mobile data traffic is growing faster than ever. Every year the demand in mobile broadband communications increases as more and more users subscribe to mobile broadband package. The amount of traffic has been doubling each year during the last few years with the increasing popularity of smartphones, super-phones and tablets with powerful multimedia capability and the necessity to reach data services and applications on mobile broadband [1, 2]. Global mobile data traffic grew 74% in 2015, 4000-fold over the past 10 years and almost 400-million-fold over the past 15 years. In the same year, more than half a billion mobile devices and connections were added [3] and an astounding 1000-fold in data traffic is expected in this decade [4].

Long Term Evolution-Advanced (LTE-A) has been recently standardized by the Third Generation Partnership Project (3GPP), but nevertheless industry and academia are working together to meet the capacity demand for mobile communication system. Several large scale project such as Mobile and wireless communications Enablers for Twenty–twenty Information Society (METIS) and 5GNOW have also recently started to investigate 5G mobile communication system, ranging from new radio access interfaces to new system architectures [5]. 5G network will have increased capacity, high data rate, low latency, reliability, scalability, flexibility [6, 7] and significant improvement in communications Quality of Service (QoS) in order to fulfil the growing demand for mobile connectivity (more than 50 billion devices are expected to be connected in 2020). To solve the aforementioned challenges, it becomes essential to adopt a network infrastructure that can efficiently integrate various wireless technologies and to enable inter-networking of existing and newly-deployed technologies [8]. 5G will realize networks capable of providing zero-distance connectivity between people and connected machines in a truly connected society with unlimited access of information for anyone, anywhere, and anytime [9]. In order to fulfil these requirements, 5G network should adopt a heterogeneous architecture with different types of cells (macrocells, small cells, and relay nodes) [10], multiple radio access technologies (RATs), massive multiple input multiple output (MIMO) at Base Stations (BSs) and/or user equipments (UEs) that will support microwaves and mmWave frequency bands [8].

It has been shown that a significant number of users accessing wireless broadband services while riding vehicles and this number is increasing significantly because of the high penetration of UEs. Users are expecting similar experience at home, in the office, when stationery or travelling. In literature, a group of users who accessing the mobile network from inside the vehicle, is known as *vehicular users* (VUEs). A significant attention has been paid to address the issues of the VUEs because they suffer from low signal quality caused by the poor macro antenna coverage of base stations inside vehicles with metallic walls [11]. The Vehicular Penetration Loss (VPL) is one of the biggest factors that limit the performance for VUEs. According to [12], the measured VPL can be as high as 25 dB in a minivan at the frequency of 2.4 GHz, and higher VPLs are foreseeable in higher frequency bands.

Hence, the communication "on the move" exhibits a low throughput for users and a greater energy consumption.

The problem becomes more critical for users that access the mobile network on public transportation vehicles (e.g. trains, buses, or trams, etc.). In this case many users in a single moving vehicle simultaneously perform network operations such as multiple individual handovers. As a result, the network must be able to manage numerous real-time handover procedures requiring more resources, signalling overhead and reporting delays.

The METIS project has taken these issues into account. In their "Horizontal Topics", they introduce the concept of "Moving Networks" as one of the scenarios that the 5G mobile network will have to satisfy [6]. A Moving Network (MN) has to enhance and extend the coverage for many communication devices that move together.

In order to increase the vehicular users performance, also the 3GPP proposes various solutions within the Heterogeneous Network deployment, as discussed in Sect. 2.

So far, the most promising solution seems to be the combination of the concepts of mobile relay and femtocell, the so called Mobile Femtocell Architecture. In fact, several studies in literature showed that the use of the Femtocell Access Point (FAP) improves the users' throughput and extends the network coverage in indoor environment [13–15]. For these reasons, many authors [11, 16–19] suggest that the FAP can be a natural opportunity for vehicular environment in order to realise a practical implementation of the "Mobile Femtocell" [16] as a new Moving Network (MN) architecture in LTE environment. Mobile Femtocell Access Point (MFAP) is located inside a vehicle and use two antennas. The users inside the vehicle

communicate with the MFAP through an omnidirectional indoor antenna, while a larger array antenna is located outside the vehicle and permits the MFAP to communicate with the eNodeB. Consequently the vehicular penetration loss can be reduced. As far as the outdoor array antenna is concerned, an aperture with a moderate gain to large would strengthen the signal at an acceptable cost.

Unfortunately, the use of Mobile Femtocells that work in the same LTE band of the macrocells can suffer from severe QoS degradation, because of the inter-cell interference that can arise between fixed and moving cells [20, 21]. So, in according to the METIS vision that suggests to use new frequency bands in 5G system [8] to increase the system capacity, we propose to adopt the mmWave technology for the in-vehicle communications, creating the Hybrid Mobile Femtocells that use both mmWave and LTE band in order to reduce the interference issues. mmWaves are currently been used for high speed Line of Sight (LOS) links and they are considered as the main technology for the next-generation mobile communication systems [22–24].

The benefits of applying the mmWave approach in in-vehicle link between users and the MFAP, are as follows:

- users inside the public vehicles will take advantage of strong short range signal transmitted by the MFAP;
- some interference issues will be solved because the nodes will use different frequency bands;
- greater throughputs will be available to vehicular and macrocell users.

In this paper we investigate the use of Hybrid-Mobile Femtocell Access Point (H-MFAP), a new approach already introduced by the authors in [20, 21]. In details, in this paper, we will assess if the adoption of H-MFAP can be really considered an effective and viable solution to the future MN. In particular, in the following, we will improve our system throughput model and we will evaluate the use of H-MFAP in different cell deployments, considering also the next HetNets, suitable for urban scenario.

The paper is organized as follows. In Sect. 2 we discuss about the different implementations of a Moving Network (MN) addressed in literature and the last researches regarding the hybrid architecture based on mmwave-technology for next 5G Networks. The issues of Mobile Femtocells that use LTE technology are discussed in Sect. 3. Our proposal is presented in Sect. 4. Section 5 describes the system models adopted for sub-urban and urban scenarios. In order to compare several MFAP solutions a new throughput model is introduced in Sect. 6. The simulation results are shown in Sect. 7. Finally, Sect. 8 concludes our work.

2 Related works

Different types of low power cells (pico eNodeB, remote radio heads, fixed relay nodes, moving relay nodes, home eNodeB) deployed under the coverage of macro eNodeBs constitute a Heterogeneous Network (HetNet) with the aim to meet the capacity need in specific hot spot area [25]. This architecture is widely considered in 5G standardization, in particular for supporting a very dense deployments of wireless communication links in urban environments, where the small cells can meet the capacity needs in specific hot spot area while the macrocells provide basic coverage.

HetNet deployment is recommended by 3GPP that propose in [26] different solutions of this architecture in order to increase the performance of the VUEs. Let's analyse them in detail:

Dedicated deployment of macro eNodeB

When the route of a public transportation vehicle is known, the coverage of macro base stations can be enhanced by deploying dedicated eNodeBs with directive antennas, along the trains lines or highways. To reduce UE handover failure rate, to extend coverage and capacity, and to reduce costs, a HetNet deployment can be used in this scenario with the use of high-power cells (eNodeB) and fixed low-power cells. The eNodeBs can be configured as the serving node, while low power nodes provide high data rates. It is necessary to coordinate the operations of the cells. Different approaches could be possible, such as Carrier Aggregation (CA), in which the high power cells transmit the Primary Component Carrier (PCC) while the Secondary Component Carrier (SCC) is transmitted by the low-power nodes, or by using cross-carrier scheduling schemes. However, the VPL remains an issue because it can't be reduced in this solution due to the presence of outdoor fixed access points. Moreover site acquisition, deployment, maintenance are a challenge for operators especially in urban scenarios [19].

Dedicated deployment of macro eNodeB + L1 repeaters

Layer 1 repeaters amplify and forward signals in a certain frequency band. In a public transportation vehicle if the RX and TX antennas are well isolated (i.e. inside vs. outside the vehicle), the repeaters can work in full-duplex mode, by using the same frequency band inside and outside the vehicle. In this way the VPL can be reduced, and the VUE can transmit data with lower power. Since the repeaters do not re-generate the received signal, the SINR cannot be improved because the L1 repeaters amplify both noise and desired signal. Moreover the core network does not control them, so the handover of the VUEs will be performed individually. In

dense deployment scenarios, the L1 repeaters may bring more interference into the system [19].

LTE as backhaul, Wi-Fi as access on board

Nowadays, the use of WiFi Access Point on board is highly popular. It consists of a WiFi hotspot that uses LTE for backhaul. All VUEs can use this node only for data connections or VOIP calls, while continuing to use the cellular network for voice calls. VPL can be avoided, group handover can be used, but only for data traffic. This solution also enables any Wifi-only devices to use LTE network as backhaul, but without authentication, security and QOS support offered by the core network. Moreover, as the WiFi operates on the open industrial, scientific and medical radio (ISM) bands, the interference issues cannot be coordinated [19].

Mobile relay node deployment

The mobile relay node (MRN) are base stations/access point mounted on vehicles. It uses two antennas: one outside the vehicle, used for the connection to the Donor eNodeB (DeNB) via LTE Un radio interface, while the users inside the vehicle communicate with it through an omnidirectional indoor antenna, consequently the VPL is eliminated. MRN may support multi-RAT functionalities, so VUEs can be connected to it through different air interface technology, e.g. LTE/3G/2G. Authors in [16] propose to communicate via LTE in both link (to the DeNB and to VUEs), so they combine the concepts of relay node and femtocells as an implementation of MRN in a so called Mobile Femtocell Access Point (MFAP) architecture. It provides eNodeB functionality and supports a subset of the UE functionality to connect to the DeNB. Using MFAPs, vehicular users may obtain high coverage and more system capacity. MFAP provides uninterrupted connectivity for the user plane and control plane of the served UEs, moreover, the drop calls and the signal overhead are reduced because the MFAP creates its own cells within a vehicle. So, it and its associated users are viewed as a single unit by the eNodeB that can perform a single group handover for all users connected to it [27]. A further advantage is the energy saving on UE: battery life can be extended thanks to shorter communication range with MFAP. Moreover, the outdoor array antenna gain strengthens the received signal.

Therefore, so far, the most promising solution to Moving Networks seems to be the MFAP architecture. To the best of our knowledge, all most recent researches exclusively adopt the LTE technology both in backhaul link and inside vehicle, but several unresolved issues arise. In details, in [17–19, 28] the potential advantages of the use of LTE-based MFAP in vehicular environment in terms of coverage and spectral efficiency have been investigated. In [29–31] the authors propose solutions for handover procedures in the Mobile Femtocell Networks. Authors in [11, 16, 32] focus on the problems of interference and propose different resource allocation schemes. The resource allocation is itself a challenging problem in cellular networks. For achieving high system throughput, it is necessary to satisfy two dual conditions: maximizing the spectral efficiency and minimize interference. If finding a good compromise between these two opposing requirements is already difficult in the case of fixed femtocells, it would be more challenging for mobile femtocells to maintain high network performance. Authors [16–19] suggest that higher performance can be obtained by reusing the macrocell frequency band in the MFAP coverage area. In this way a higher spectral efficiency could be obtained, but it must handle the channel interference issues caused by the use of the same resources. This problem is expected to become more significant in the near future due to the large deployment of fixed and moving small cells. In fact, reusing the same bands within the small cells and concurrently handling interference problem are dramatically difficult, especially with moving cells.

Regarding mmWave communications, several studies propose the use of mmWave spectrum (between 30 and 300 GHz) as a key enabler to provide multi-gigabits-per-second data rates over short distances for 5G wireless networks. Most of the current research is focused on the 28, 38, 60 GHz band, and the E-band (71–76 and 81–86 GHz). Both industry and academia are working for standardization activities in wireless area network, such as IEEE 802.15.3 Task Group 3c (TG3c) [33], IEEE 802.11ad standardization task group [34], Wireless HD Consortium, Wireless Gigabit Alliance (WiGig) [22] (this is an industry consortium devoted to the development and promotion of wireless communications in the 60 GHz band). There are several on going research projects such as FP7 EU Project METIS [6] in which the adoption of mmWave network in 5G [35] is being evaluated to be used in small cell access, cellular access and wireless backhaul [36]. More specifically, to fully utilize the mmWave spectrum, 5G is expected to adopt hybrid architectures for Heterogeneous Network, where mmWave small cells are overlaid onto a conventional macro-cellular network [23, 24, 37]. In [24], a RAN (Radio Access Network)-level tightly coupled interworking solution is proposed for the implementation of LTE/WiGig mm-wave HetNets, which is much more prospective compared to conventional interworking architectures. In [37], the envisioned HetNet comprises a conventional macro-cellular network and novel small cells that use the mmWave both for backhaul and access. In addition, in [37] the concept of control plane (CP) and user plane (UP) splitting HetNet is also introduced, where the CP is

provided by a conventional macrocell to deliver broad coverage, while the UP data are provided by mmWave small cells. This architecture enables continuous connectivity with capacity boosting by using the advantages of both the macrocell and the "fixed" small cells.

However, to date, no work in literature proposes a hybrid architecture based on LTE/mmwave technology as a solution for next Moving Networks, where severe and different interference issues can arise.

3 Issues on LTE–MFAP

In the following we consider a macrocell with public busses equipped with MFAP devices. We specify two kinds of mobile users: out_UE, user equipment outside the vehicles and served by the eNodeB; VUE, user equipment inside the vehicles. According to 3GPP convention, the MFAP system distinguishes three kinds of links (see Fig. 1): "backhaul link", the link between the DeNB and MFAP; "access link", the link between the MFAP and the VUE; "direct link", the link between the eNodeB and the out_UE.

For a pure LTE MFAP (L-MFAP), the backhaul and access links are based on LTE radio access. We focus on downlink communications. The MFAP decodes and buffers data received from the backhaul link and then forwards them to the VUEs. These two phases can't be done at the same time. In order to reduce the interference that may arise between the transmissions on access and backhaul links, a time division scheme for these two transmissions can be adopted as an easier and a more natural solution.

At this regard, [16, 17] propose the use of a time interval for the simultaneous transmissions on the backhaul and direct links, and another interval for transmission on the access and direct links. In the first interval, due to the fact that the MFAP is seen as an out_UE from the eNodeB and the orthogonal nature of OFDMA, there is no interference between backhaul and direct links. In the second interval, due to the simultaneous transmissions by two nodes

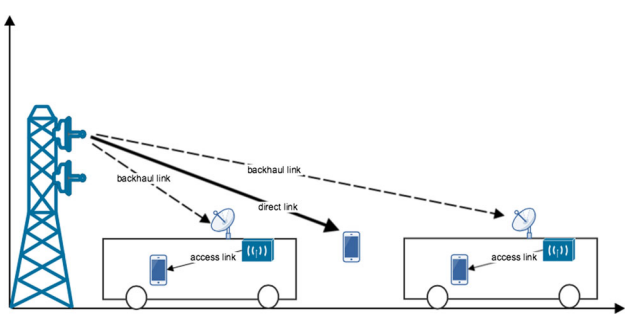

Fig. 1 MFAP architecture with the different names of the links

(eNodeB and MFAP), appropriate resources allocation policies are required. In [16], two resource partitioning schemes are investigated:

- an orthogonal partitioning scheme in which the whole system bandwidth is divided in two different sub-bands, one for each node;
- a non-orthogonal scheme in which the whole bandwidth can be simultaneously used by both nodes.

In the first scheme there is no interference, but it has the drawback of a poor spectral efficiency due to the subset of orthogonal frequencies that can be used. For this reason, the orthogonal partitioning scheme appears to be anachronistic in a 5G system where more and more capacity is required. In the second scheme, the out_UEs and VUEs use the same LTE bandwidth and the same technology. In this way the resource utilization is improved and the Radio Resource Management is more flexible than the first scheme. However, it introduces intra-cell interference between the users of access and direct links. In this paper, we evaluate how these interference issues affect the performance of the system in different scenarios. We will show that the interference caused by the direct link transmission on the access link, is negligible when the MFAP moves away from the eNodeB site. In this case, since the eNodeB signal strength is poor, the metal walls of public transportations insulate it from external transmissions. Conversely, the interference caused by the access link transmissions on the direct link is always remarkable.

These restrictions become burdensome in a real-scenario where the MFAP moves around a city. In literature [16, 18, 28, 32], the use of L-MFAPs is recommended only in half and edge of the cell. In particular, when the bus is approaching the eNodeB site, VUEs served by the L-MFAP measure a low SINR. So, in [16], it is suggested that they will be forced to disconnect from L-MFAP and to switch to eNodeB. Unfortunately this results in a high number of simultaneous handovers. Moreover, as the bus moves, as soon as the signal of the MFAP becomes acceptable, users will have to re-engage with the MFAP causing additional handover procedures.

Analogously, in [28] the authors suggest that out_UEs, far away from their serving eNodeB and in proximity of a bus, could trigger a handover toward MFAP. However, because this connection is active only for a short time, depending on the speed of the bus, this event can determine QoS degradation and call dropping.

In conclusion the solutions proposed so far in the literature exhibit a high performance only in limited scenarios. They do not take into account that in real operating conditions, the system could suffer from severe QoS degradation in terms of global throughput and/or signalling load.

4 Hybrid MFAP

In order to guarantee the use of MFAP as Moving Network in all conditions, regardless of the proximity to the eNodeB or other MFAPs, we propose a new MRN architecture that uses LTE technology to communicate with eNodeB in the backhaul link, and to adopt mmWave inside the vehicle for the access link. Hybrid-MFAP (H-MFAP) is the name of our new concept of MFAP for a MRN implementation. However, several aspects need to be examined so the use of H-MFAP can be really considered an effective and viable solution. What frequency band is more suitable? Is it available? Is the technology ready? Are the performance as we expect?

As already mentioned, most of the current research is focused on the 28, 38, 60 GHz band, and the E-band (71–76 and 81–86 GHz). There are many differences between the mmWave communications and the microwaves bands, so there are many challenges in physical, medium access control and routing layers due to the free space propagation loss, atmospheric impairments and oxygen loss factors. As an example, a signal at 60 GHz has an attenuation due to free space loss of almost 36 dB higher than a signal at 1 GHz, without considering the atmospheric loss and the oxygen absorption [54]. These loss factors become relevant for mmWave links exceeding 100 m and crucial for longer distance like 1 km [38]. For these reasons, authors in [22], in the framework of 5G, suggest to use mmWave in outdoor scenarios for access link in small cells and backhaul with distance less than 300 m.

In particular, the 60 GHz band and the E band (71–76 and 81–86 GHz) are better suited to tackle the mobile data challenge since larger bandwidths are available, they are license free or light-licensed, and they are available almost worldwide.

In recent years, many products based on 60 GHz frequency have been introduced on the market: chipsets and transceivers for a variety of applications (indoor, backhaul…) [39–47, 55] are commercially available, showing that the 60 GHz technology is already accessible.

Consequently on the above observances and by considering that VUEs are in indoor environment with short-range links, we propose to use 60 GHz-mmWave in the access link of a H-MFAP. In this way, thanks to the addition of the new frequency band, we solve the interference problems with other technologies that uses LTE. In summary, there are several advantages using the 60 GHz bands: highly secure operations thanks to the short transmitting range, high-speed links (wireless fiber), high level of frequency re-use enabled, mature technology (this spectrum has a long history of being used for secure communications), carrier-class communication links enabled with 99.999% of availability [48], large bandwidth available (from 56 to 66 GHz in Europe). If we consider Shannon's capacity formula, the sheer capacity of a mmWave system is considerable. As a result, large band interval per channel can be allocated (e.g. 220 MHz or more compared with 5–20 MHz in today's microwave system [21]). New design guidelines are proposed for this technology: the small wavelength at 60 GHz frequency makes it possible to pack a large number of antennas into small size and low power transceivers, where the use of the MIMO techniques can enhance spectral efficiency [49].

5 System model

In the following sections, we want to analyse the performance achievable with the adoption of mmWave-based MFAP (H-MFAP) compared to those exhibited by L-MFAP. In order to carry out a more thorough investigation, we consider two significantly different configurations of cells deployment for Sub-urban and Urban scenarios. In both scenarios we make the following assumptions:

- the H-MFAPs use a dual mode technology, mmWaves for the access link and LTE for the backhaul link;
- for the mmWave radio access in H-MFAP, we consider a carrier of 60 GHz and a bandwidth of 220 MHz as in [22];
- the UEs are equipped with transceiver of multi-standard technologies (e.g. mmWave and LTE). When a UE gets on a bus equipped with H-MFAP, it performs a handover procedure to the mmWave technology.

In the "Sub-urban" scenario the area is covered by contiguous macrocells where we consider that:

- the access and the backhaul link use the same LTE band with a carrier at 2.6 GHz;
- any MFAP in the backhaul link communicates to DeNB by means LTE Resource Blocks (RBs) with a carrier of 2.6 GHz and this link has an Antenna Gain over the direct link;
- the L-MFAP deployed in a bus can operate in non-orthogonal or orthogonal allocation schemes;
- there are a number of out_UEs in a macrocell area served by the eNodeB by means of a direct link in LTE at 2.6 GHz.

In an "Urban" Scenario, in order to fulfil the requirements of capacity and coverage, a dense deployment of small cells embedded in a macrocell will be necessary. Due to the dense deployment of HetNet in this context, in order to reduce the inter-cell interference, we consider, as in [5], that small cells (femtocells and picocells) coexist and work

in the same LTE bandwidth (2.6 GHz band), while the eNodeB of the macrocell transmits in the 800 MHz band. In this topology, we assume that:

- any MFAP communicates with the DeNB by means of a backhaul link at 800 MHz;
- the access link of L-MFAP uses the LTE technology with a carrier of 2.6 GHz;
- in the macrocell area there are a number of UEs connected to the picocells (pico_UEs) that work at 2.6 GHz.

6 Performance analysis

6.1 Propagation model

For each link we consider an opportune propagation model as suggested in literature. In each one, d is the distance between the UE and its serving access point (eNodeB, MFAP or pico base station) of the path loss. Log-normal shadowing (S) is applied to all link with different standard deviation values. According to the ITU-R we used $S(\sigma_1)$ for the standard deviation of shadowing in sub-urban macro cell area (SMa), $S(\sigma_2)$ for the access link by considering the standard deviation for ITU-R Indoor Hotspot (InH) in LOS conditions, while $S(\sigma_3)$ is the value used for mmWave link [50]. The values are shown in Table 2.

The UEs connected with the eNodeB, e.g. direct links, are considered in the outdoor sub-urban environment. So, the propagation model can be modelled as follows [50]:

$$L_{direct}(d) = 15.3 + 37.6\log_{10}(d) + S(\sigma_1)[dB] \quad (1)$$

For the backhaul link, the path loss model used is the same of the direct link (1) considering also the Antenna Gain (Ag):

$$L_{backhaul}(d) = 15.3 + 37.6\log_{10}(d) - Ag + S(\sigma_1)[dB] \quad (2)$$

The LTE access link is modelled with a model as in [29]:

$$L_{access}(d) = 20\log_{10}(f_{MHz}) + 28\log_{10}(d) - 28 + S(\sigma_2)[dB] \quad (3)$$

where f_{MHz} is the LTE carrier frequency.

For the access link in mmWave technology we consider the propagation model as in [51]:

$$L_{mmWave}(d) = PL_0 + 10 \cdot \alpha \cdot \log_{10}(d) + S(\sigma_3)[dB] \quad (4)$$

where PL_0 is the free space Path Loss at 1 m (68 dB at 60 GHz), α is the exponential factor, equals 2.17 for a Line-of-Sight indoor hall.

In an urban scenario, we consider the presence of the picocell base stations. The link between the pico_UEs and its serving cell, is modelled as in [50]:

$$L_{pico}(d) = 30.6 + 36.7\log_{10}(d) + S(\sigma_4)[dB] \quad (5)$$

where Log-normal shadowing effect is modelled by considering a standard deviation of the ITU-R urban microcell (UMi) model, $S(\sigma_4)$.

6.2 SINR calculation

For each UE we estimate the SINR as the ratio between the signal power received from its serving Cell (Macrocell, Femtocell, Picocell), and the total interference power due to the co-channel transmissions plus the Thermal Noise (N).

In the following formulas, Lw_1 or Lw_2 are the attenuation experienced by signals entering the vehicle when LTE or 60 GHz link are considered, respectively.

For convenience, we use the following notation $SINR_y^x$ to indicate the SINR measured in the link $\boldsymbol{y}$ (y may assume the values D, A, B, that stand for: Direct, Access, Backhaul) using the solution $\boldsymbol{x}$ (x may assume the values W, O, N, H, that stand for: Without MFAP; *L*-MFAP with Orthogonal allocation scheme; L-MFAP with Non-orthogonal allocation scheme; H-MFAP). Let's note that in some cases the interference is zero, but we maintain the same notation (SINR) for homogeneity.

The SINR measured by the MFAP in the backhaul link is equal to:

$$SINR_B = \frac{P_1 \cdot L_{backhaul}(d_{j,e})}{N} \quad (6)$$

where P_1 is the transmission power of the eNodeB, $d_{j,e}$ is the distance in meters between the MFAP j and the donor eNodeB e. Please note that we do not have interference because we are considering a single macrocell where the MFAP is viewed as an out_UE by the eNodeB, so it has been assigned orthogonal resources like the other UEs.

The SINR measured by an VUE without MFAP is calculated as follows:

$$SINR_e^W = \frac{P_1 \cdot L_{direct}(d_{m,e}) \cdot Lw_1}{N} \quad (7)$$

where, $d_{m,e}$ is the distance in meters between the eNodeB e and the UE m. Again, we have not to considerate any interference because in a single macrocell scenario, all the UEs have orthogonal resources assigned by the OFDMA mechanism.

6.2.1 *Calculation of SINR when the access link operates in LTE mode with orthogonal allocation scheme*

The L-MFAP that operates in orthogonal allocation scheme does not suffer from the interference issues due to

the frequency band reuse. So, for an out_UE, the SINR in direct link is calculated as:

$$\mathrm{SINR}_{\mathrm{D}}^{\mathrm{O}} = \frac{\mathrm{P}_1 \cdot \mathrm{L}_{\mathrm{direct},}\left(\mathrm{d}_{\mathrm{n,e}}\right)}{\mathrm{N}} \tag{8}$$

where $d_{n,e}$ is the distance in meters between the eNodeB e and the out_UE n.

The SINR for a VUE served by the L-MFAP k, is calculate as follows:

$$\mathrm{SINR}_{\mathrm{A}}^{\mathrm{O}} = \frac{\mathrm{P}_2 \cdot \mathrm{L}_{\mathrm{access}}\left(\mathrm{d}_{\mathrm{m,k}}\right)}{\mathrm{N}} \tag{9}$$

where P_2 is the transmission power of the L-MFAP; $d_{m,k}$ is the distance in meters between the VUE m and the L-MFAP k.

6.2.2 Calculation of SINR when the access link operates in LTE mode with non-orthogonal allocation scheme

The SINR of the direct link for an out_UE n, is given by:

$$\mathrm{SINR}_{\mathrm{D}}^{\mathrm{N}} = \frac{\mathrm{P}_1 \cdot \mathrm{L}_{\mathrm{direct},}\left(\mathrm{d}_{\mathrm{n,e}}\right)}{\mathrm{I}_{\mathrm{f}} + \mathrm{N}} \tag{10}$$

In (10) the interference (I_f) due to the J neighboring L-MFAPs is:

$$\mathrm{I}_{\mathrm{f}} = \sum_{\mathrm{j}=1}^{\mathrm{J}} \mathrm{P}_2 \cdot \mathrm{L}_{\mathrm{access}}\left(\mathrm{d}_{\mathrm{n,j}}\right) \cdot \mathrm{Lw}_1 \tag{11}$$

where $d_{n,j}$ is the distance in meters between the out_UE n and the L-MFAP j.

In the access link, the VUE m, served by a L-MFAP k, measures a SINR equals to:

$$\mathrm{SINR}_{\mathrm{A}}^{\mathrm{N}} = \frac{\mathrm{P}_2 \cdot \mathrm{L}_{\mathrm{access}}\left(\mathrm{d}_{\mathrm{m,k}}\right)}{\sum_{\mathrm{j}=1,\mathrm{j}\neq\mathrm{k}}^{\mathrm{J}}\left(\mathrm{P}_2 \cdot \mathrm{L}_{\mathrm{access}}\left(\mathrm{d}_{\mathrm{m,j}}\right) \cdot 2 \cdot \mathrm{Lw}_1\right) + \mathrm{I}_{\mathrm{M}} + \mathrm{N}} \tag{12}$$

In (12) we consider the interference power I_f of the $J-1$ neighbouring L-MFAP, each at a distance of $d_{m,j}$ meters from the VUE m, and two penetration loss factors due to the presence of two walls of the neighboring buses; I_M is the interference power received from the eNodeB e given by:

$$\mathrm{I}_{\mathrm{M}} = \mathrm{P}_1 \cdot \mathrm{L}_{\mathrm{direct}}\left(\mathrm{d}_{\mathrm{m,e}}\right) \cdot \mathrm{Lw}_1 \tag{13}$$

6.2.3 Calculation of SINR when the access link operates in mmWave technology

Due to the different frequency bands used in this case, the UEs connected to the eNodeB do not suffer from the interference of the H-MFAP. The out_UE n in the direct link, measures a SINR level equal to:

$$\mathrm{SINR}_{D}^{H} = \frac{\mathrm{P}_1 \cdot \mathrm{L}_{\mathrm{direct},}\left(\mathrm{d}_{\mathrm{n,e}}\right)}{\mathrm{N}} \tag{14}$$

In the access link, we have to consider only the inter-H-MFAP interference, so the SINR for a VUE m is:

$$\mathrm{SINR}_{A}^{H} = \frac{\mathrm{P}_2 \cdot \mathrm{L}_{\mathrm{mmWave}}\left(\mathrm{d}_{\mathrm{m,j}}\right)}{\sum_{\mathrm{j}=1,\mathrm{j}\neq\mathrm{k}}^{\mathrm{J}}\left(\mathrm{P}_2 \cdot \mathrm{L}_{\mathrm{mmwave}}\left(\mathrm{d}_{\mathrm{m,j}}\right) \cdot 2 \cdot Lw_2\right) + \mathrm{N}} \tag{15}$$

where P_2 is the transmitting power of a H-MFAP in mmWave technology.

6.2.4 Calculation of SINR of the UE connected to a pico base station

In an urban scenario with a dense deployment of small cells, both L-MFAP and picocell use the same frequency LTE band at 2.6 GHz, instead the eNodeB of the macrocell transmits data in different band (800 MHz). We evaluate the SINR of the pico_UEs as follows:

$$\mathrm{SINR}_{\mathrm{pico\_UE}} = \frac{\mathrm{P}_3 \cdot \mathrm{L}_{\mathrm{pico}}(\mathrm{d}_{\mathrm{s}})}{\mathrm{I}_{\mathrm{MFAP}} + \mathrm{I}_{\mathrm{p}} + \mathrm{N}} \tag{16}$$

where P_3 is the transmitting power of a pico base station, d_s the distance between a pico_UE and its serving pico base station; $\mathrm{I}_{\mathrm{MFAP}}$ and I_{p} are the interference contributions of the nearby MFAP and picocells respectively. In particular,

$$\mathrm{I}_{\mathrm{MFAP}} = \sum_{\mathrm{j}=1}^{\mathrm{J}}\left(\mathrm{P}_2 \cdot \mathrm{L}_{\mathrm{pico}}\left(\mathrm{d}_{\mathrm{j}}\right) \cdot \mathrm{Lw}_1\right) \tag{17.a}$$

where d_{j} is the distance between the pico_UE and the interfering L-MFAP j with non-orthogonal allocation scheme;

$$\mathrm{I}_{\mathrm{MFAP}} = 0 \tag{17.b}$$

in the case of vehicles equipped with H-MFAP.

6.3 Throughput model

In the following, we propose a model in order to evaluate the maximum achievable system throughput in downlink and to compare the performance of H-MFAP with those suggested and examined in the literature so far: L-MFAP with Non-orthogonal allocation scheme, L-MFAP with Orthogonal allocation scheme, vehicle Without MFAP.

For the LTE downlink data transmissions, the base station selects a Modulation and Code Scheme (MCS) based on Channel Quality Indicator provided by mobile user. LTE specifications define several MCSs that are used depending on the radio link conditions: a higher order modulation (more bits per modulated symbol) and a higher code rate can be used only when channel conditions are

good, i.e. the SINR is sufficiently high. In our simulations we adopt the parameters of SINR requirements vs. MCS (see Table 1) presented in [52]. Please note that, as suggested in [52], we use an extra Implementation Margin (IM) for the difference in SINR requirements between theory and practical implementation.

The minimum LTE radio resource allocated to user is a Resource Block which consists of 12 subcarrier (180 kHz) assigned for 0.5 ms. We consider a LTE frame structure with normal cyclic prefix with 7 OFDM symbol per subcarrier, so there are 84 symbols per Resource Block (RB). By applying the data of Table 1, for each SINR value we can calculate the amount of bits in each RB, Q as:

$$\mathrm{Q(SINR)} = \frac{\mathrm{x\ bit}}{\mathrm{symbol}} \cdot \mathrm{code\ rate} \cdot 84 \left[{}^{\mathrm{bit}}/_{\mathrm{RB}} \right] \tag{18}$$

At the sole aim of comparing the several MFAP solutions, we can assume a fair allocation of resources to NUE greedy users (sum of all VUEs, N_{VUE}, and out_UEs, N_{out_UE}) and we evaluate the achievable maximum system throughput.

To calculate the system throughput, we consider a Transmission Time Interval (TTI) of 1 ms. Notice that, in a system with MFAPs, the transmission in the backhaul link and access link occurs in two different intervals. For simplicity, we consider that the transmissions take place in the first and the second slots of the same TTI, respectively.

Finally, it is necessary to observe that the amount of bits that a MFAP can send to VUEs in the access link is limited by the number of bits that the eNodeB has previously sent to the MFAP in the backhaul link.

For each link and solution considered, the SINR value is calculated using the Formulas in (6–15). So, the maximum system throughput calculation, Th^x, for the moving network solution x (x = W, O, N, H), can be calculated as:

$$Th^x = \sum_{i=1}^{N_{out\_UE}} \mathrm{Th}_{\mathrm{out\_UE,i}} + \sum_{j=1}^{J} \sum_{k=1}^{N_{VUE,j}} \mathrm{Th}_{\mathrm{VUE,jk}} \tag{19}$$

where J is the number of MFAP considered and $N_{VUE,j}$ the number of VUEs located in the vehicle with the $MFAP_j$: Based on previous assumptions and observations, we have derived the $Th_{out\_UE,i}$ and $Th_{VUE,jk}$ in the following formulas for all the cases considered.

6.3.1 Without MFAP

In a configuration without MFAP the terms of (19) are calculated as follows:

$$Th^{W}_{out\_UE,i} = \frac{N_{RB}}{N_{UE}} \left\{ \frac{\mathrm{Q}\left(\mathrm{SINR}^{\mathrm{W}}_{\mathrm{D,i}}\right)}{0.5 \cdot 10^{-3}} \right\} \tag{20}$$

$$\mathrm{Th}^{\mathrm{W}}_{\mathrm{VUE,k}} = \frac{N_{RB}}{N_{UE}} \left\{ \frac{\mathrm{Q}\left(\mathrm{SINR}^{\mathrm{W}}_{\mathrm{e,k}}\right)}{0.5 \cdot 10^{-3}} \right\} \tag{21}$$

where N_{RB} is the total number of Resource Blocks for the considered LTE system bandwidth. To calculate (20) and (21), we have considered one time slot (0.5 ms) and that all RBs are fairly allocated to the N_{UE} users. Therefore, we have evaluated the amount of bits per RB sent to each user depending on relative SINR measured.

6.3.2 L_MFAP with Orthogonal allocation scheme

$$\mathrm{Th}^{\mathrm{O}}_{\mathrm{out\_UE,i}} = \frac{N_{RB}}{N_{UE}} \left\{ \frac{2 \cdot \mathrm{Q}\left(\mathrm{SINR}^{\mathrm{O}}_{\mathrm{D,i}}\right)}{10^{-3}} \right\} \tag{22}$$

Table 1 Downlink SINR requirements for LTE

Modulation	Code rate	SINR (dB)	IM (dB)	SINR + IM (dB)
QPSK (2 bit/symbol)	1/8	−5.1	2.5	−2.6
	1/5	−2.9		−0.4
	1/4	−1.7		0.8
	1/3	−1		1.5
	1/2	2		4.5
	2/3	4.3		6.8
	3/4	5.5		8.0
	4/5	6.2		8.7
16QAM (4 bit/symbol)	1/2	7.9	3	10.9
	2/3	11.3		14.3
	3/4	12.2		15.2
	4/5	12.8		15.8
64QAM (6 bit/symbol)	2/3	15.3	4	19.3
	3/4	17.5		21.5
	4/5	18.6		22.6

$$\mathrm{Th}^{\mathrm{O}}_{\mathrm{VUE,jk}} = \frac{\mathrm{N_{RB}}}{\mathrm{N_{UE}}} \left\{ \frac{\min\left[\mathrm{Q}\left(\mathrm{SINR_{B,j}}\right), \mathrm{Q}\left(\mathrm{SINR^{O}_{A,jk}}\right)\right]}{10^{-3}} \right\} \tag{23}$$

For deriving Eq. (22), we have considered that for each RB bandwidth assigned to the out_UE$_i$, the eNodeB in 10^{-3} ms (two time slots) can transmit two different data blocks to out_UE$_i$. Instead in (23), the amount of bits received by each VUE$_{jk}$ is the minimum between the amount of bits that its serving MFAP$_j$ has previously received in the backhaul link and those it could send in the access link.

6.3.3 L_MFAP with Non-orthogonal allocation scheme

$$\begin{aligned} Th^{N}_{out\_UE,i} &= \frac{1}{10^{-3}} \left[\frac{\mathrm{N_{RB}}}{\mathrm{N_{UE}}} \left(\mathrm{Q}\left(\mathrm{SINR^{N}_{D,i}} \right) \right) \right. \\ &\quad \left. + \frac{\mathrm{N_{RB}}}{\mathrm{N_{out\_UE}}} \left(\mathrm{Q}\left(\mathrm{SINR^{N}_{D,i}} \right) \right) \right] \\ &= \frac{\mathrm{N_{RB}}(\mathrm{N_{out\_UE}} + \mathrm{N_{UE}})}{\mathrm{N_{UE}} \cdot \mathrm{N_{out\_UE}}} \frac{\mathrm{Q}\left(\mathrm{SINR^{N}_{D,i}} \right)}{10^{-3}} \end{aligned} \tag{24}$$

$$Th^{N}_{VUE,jk} = \frac{1}{10^{-3}} \left\{ \min \left[\frac{\mathrm{N_{RB}}}{\mathrm{N_{UE}}} \mathrm{Q}\left(\mathrm{SINR_{B,j}}\right), \frac{\mathrm{N_{RB}}}{\mathrm{N_{VUE,j}}} \mathrm{Q}\left(\mathrm{SINR^{N}_{A,jk}} \right) \right] \right\} \tag{25}$$

In this case, in the second time slot, each access point (eNodeB and L-MFAP) disposes of the whole bandwidth ($\mathrm{N_{RB}}$) that can fairly allocate to its connected UEs. So, in the access link, each L-MFAP has more RBs available for sending the amount of bits that it has received in the backhaul link in the previous time slot.

6.3.4 H-MFAP

$$\mathrm{Th}^{\mathrm{H}}_{\mathrm{out\_UE,i}} = \mathrm{Th}^{\mathrm{N}}_{\mathrm{out\_UE,i}} \tag{26}$$

$$\mathrm{Th}^{\mathrm{H}}_{\mathrm{VUE,jk}} = \min \left[\frac{\mathrm{N_{RB}}}{\mathrm{N_{UE}}} \frac{\mathrm{Q}\left(\mathrm{SINR_{B,j}}\right)}{10^{-3}}, \frac{\mathrm{Th^{H}_{A}}}{\mathrm{N_{VUE,j}}} \right] \tag{27}$$

where Th^{H}_{A} is the total throughput in the mmWave access link shared by VUEs connected to the H-MFAP$_j$. The throughput calculation for H-MFAP solution is analogous to that for L-MFAP with non-orthogonal allocation scheme, except, obviously, for the access link. Please note that the mmWave radio access has not yet been standardized. However, some studies presented in literature [22, 23, 49] provide the achievable throughput values in function of the SINR measured by the UE.

7 Simulation results

In this section we present the results of our analysis. We compare the performance of our MFAP solution, H-MFAP, with other solutions proposed in literature, by means of Matlab simulations. The system parameters are shown in Table 2.

7.1 Scenario "Sub-urban"

We consider a single bus equipped with a MFAP that moves with constant velocity in a macrocell area. The bus starts its route near the eNodeB, then moving away, accosts to a greedy out_UE, located at 100 m from the eNodeB. Inside the bus there is a single greedy VUE distant 5 m from the MFAP. Both eNodeB and MFAP transmit with constant power per Resource Block. Firstly, we focus on SINR measured by the VUE. Figure 2 shows the SINR levels measured in the backhaul and access links. When the vehicle is more than 200 m from the eNodeB, any solution with MFAP exhibits higher values of SINRA than those without MFAP, SINR^{W}_{e}. These results reinforce the need to use Moving Networks. However, not all MFAP schemes ensure high performance in a realistic and dynamic scenario. In fact, while the performances of L-MFAP with Orthogonal scheme and H-MFAP are constant, the SINR^{N}_{A} degrades significantly when the bus is near the eNodeB site. This is because the eNodeB signal strength is too high and the metal walls of the bus are not able to insulate the vehicle. Only if the MFAP moves far away from the

Table 2 System parameter

Parameter	Symbol	Value
LTE bandwith		10 MHz
mmWave bandwith		220 MHz
Transmit power of eNodeB	P_1	46 dBm
Transmit power of MFAP	P_2	23 dBm
Transmit power of MFAP	P_3	23 dBm
Speed buses	v	20 m/s
Wall penetration Los in LTE	Lw_1	20 dB
Wall penetration Los in mmWave	Lw_2	40.1 dB
MFAP antenna gain	A_g	8 dB
Noise figure in LTE	NF_1	5 dB
Noise figure in mmWave	NF_2	8 dB
Shadowing standard deviation for SMa	σ_1	6 dB
Shadowing standard deviation for InH	σ_2	3 dB
Shadowing standard deviation for mmWave	σ_3	0.88 dB
Shadowing standard deviation for UMi	σ_4	7 dB

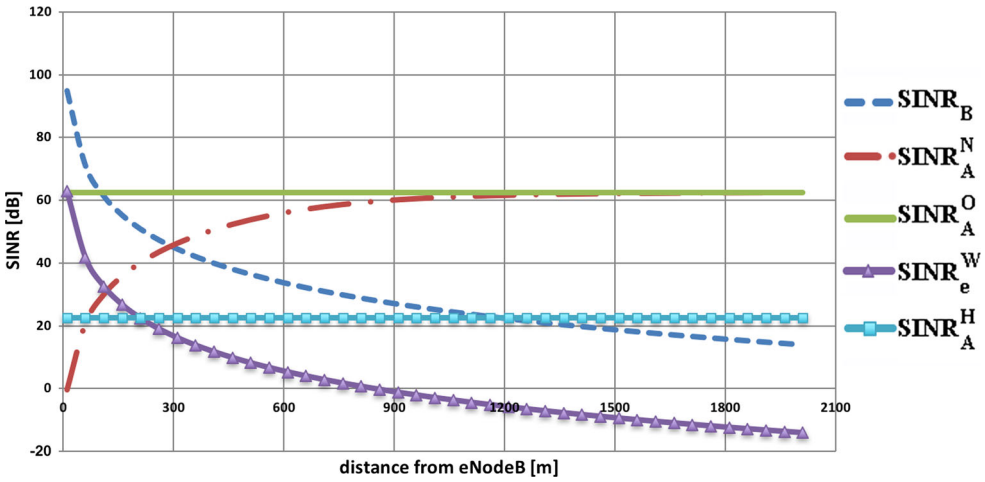

Fig. 2 SINR in dB measured in backhaul (*dotted line*) and access link in different configuration of MFAP: non-orthogonal scheme (*line with dots* and *dashes*), orthogonal scheme (*solid line*), in a configuration without MFAP (*line with triangles*) and with H-MFAP (*line with square*)

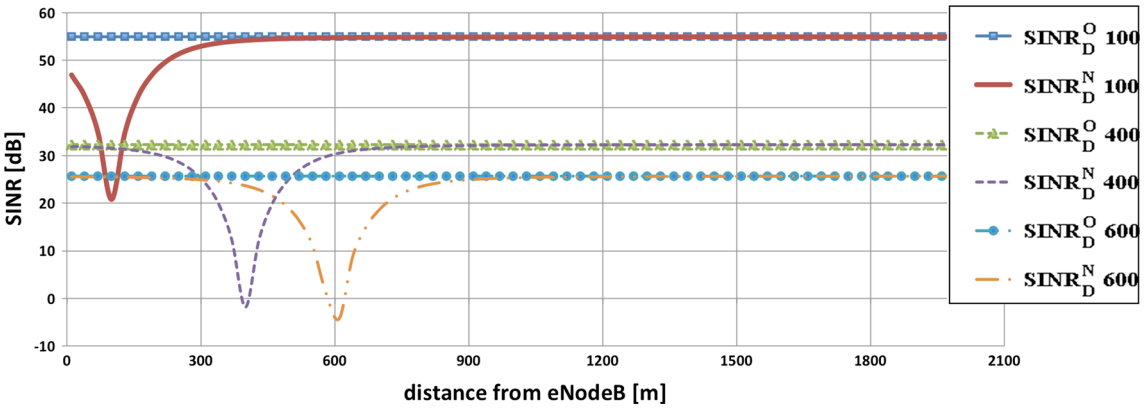

Fig. 3 SINR measured in the direct link versus different out_UE positions by benchmarking the L_MFAP with orthogonal and non-orthogonal allocation scheme

eNodeB, the interference on access links due to the direct link transmissions becomes negligible. Also, Fig. 2 shows that the constant SINR_A^H value is almost always less than SINR_A^N and SINR_A^O values, but its value is high enough for not limiting the maximum achievable throughput. In fact, in our simulation the value of SINR_A^H equals 22.64 dB, that is more than 21 dB, enough for a VUE to obtain a data rate of 990 Mbps, as proved in [22]. This value is considerably higher than the maximum throughput achievable in LTE-based backhaul link. So, the calculation of Th_{VUE} in Eq. (27) depends only on the backhaul link throughput.

In Fig. 3 we show the SINR_D values measured when the single out_UE is at 100, 400, or 600 m away from the eNodeB and the minimum distance from the MFAP is 10 m in any case considered. Obviously the proximity of vehicle equipped with H-MFAP or L-MFAP with orthogonal allocation scheme does not affect the constant SINR_D value measured by out_UE. Instead the proximity of L-MFAP with non-orthogonal scheme always results significant. The SINR_D^N value notably decreases when the bus passes near the out_UE. This is because the LTE antenna inside the bus cannot have high directivity and, consequently, the signal strength is sufficiently high to cross the metal walls and interfere with the direct links.

In Fig. 4, we compare the measurements of the maximum achievable throughput by the entire system for each solution, using the formulas (19–27) derived in our analysis. When the vehicle without MFAP moves away from the eNodeB, the throughput rapidly decreases already by 300 m of distance. This is because the eNodeB signal reaches the VUE too weak ($\text{Th}_{\text{VUE}} \rightarrow 0$) and only the out_UE can exploit the resources of him allocated, so the total throughput reaches only 50% of maximum capacity. In the case of L-MFAP with orthogonal allocation scheme, the system is able to guarantee a throughput to VUE up to 1200 m, but with a waste of 25% of resources that increases with the increasing of the number of MFAPs. It represents a high price to pay in contrast with one of the 5G requirements that is the increase of the spectral efficiency. In the case L-MFAP with non-orthogonal allocation

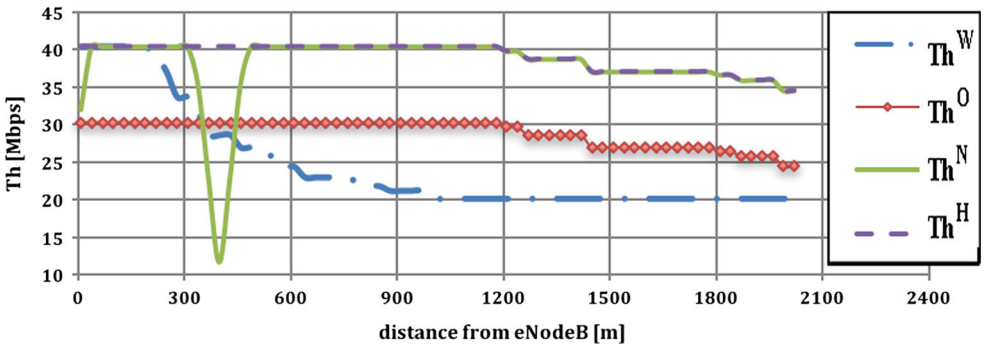

Fig. 4 Overall system throughput in a scenario without MFAP (*line with dots* and *dashes*), with L-MFAP with orthogonal allocation scheme (*line with triangles*), with non-orthogonal allocation scheme (*solid line*), and with H-MFAP (*dashed line*)

scheme, the system can work at its full capacity, but under specific restrictions: the MFAP must move away from eNodeB and out_UEs. In fact, the performance degrades significantly when the vehicle is close to eNodeB (Th_{VUE} is almost zero up to 50 m) and when the vehicle passes near an out_UE that causing a drastic reduction of Th_{out_UE}.

Finally, the H-MFAP outperforms both L-MFAP allocation schemes. In fact, the H-MFAP presents an overall increase in throughput of 33% compared to the orthogonal scheme and it does not suffer from severe limitations to its proximity to the eNodeB and out_UEs, as shown in L-MFAP with non-orthogonal allocation scheme.

Please note that, when the vehicle exceeds 1200 m of distance from eNodeB, the total throughput degrades with any investigated solutions. This is because, despite the additional gain of the external MFAP antenna, the SINRB decreases under the values of 22.6 dB, i.e. the minimum requirement to apply the MCS that ensures the highest throughput (see Table 1). As a result, from this distance onwards, the Th_B represents an upper bound for the Th_{VUE}.

We also examined whether and how the presence of two nearby vehicles equipped with MFAPs can affect the performance of the system. The simulation results show that, thanks to the double penetration loss due to the two bus walls (see Eqs. 12 and 15), in no case investigated it has been measured a significant inter-MFAP interference that can alter the performance for VUEs. Instead, in the only case of L-MFAP with non-orthogonal scheme, the out_UE throughput is further degraded by the presence of two nearby L-MFAPs. For example, when a greedy out_UE is located at 100 m from the eNodeB and 10 m from a L-MFAP, the system throughput is 35.28 Mbps and decreases until 30.24 Mbps if another vehicle equipped with L-MFAP approaches, as shown in Fig. 5.

7.2 Scenario "Urban"

In the previous sub-section, we have seen the better performance of L-MFAPs in non-orthogonal allocation scheme than those that work in orthogonal scheme. For this reason, in the following, we only consider L-MFAP with non-orthogonal allocation scheme.

Firstly we examine the VUE performance when a vehicle equipped with a L-MFAP moves in a picocell area at different distance d from the pico base station. We want to evaluate the inter-cell interference between a VUE and a pico_UE that use the same RB assigned by own serving base station.

The $SINR_A$ measured by a VUE is shown in Fig. 6. As we expected, the $SINR_A$ decreases when the L-MFAP is near to a pico base stations, however, thanks to the insulating effect of the VPL and the lower transmitting power of a pico base station than those of a eNodeB, its value is high enough (58.6 dB) to achieve the maximum bit rate in according to MCS (see Table 1). Moreover, as already seen in "sub-urban" scenario, the presence of two nearby MFAPs does not affect the performance of the VUEs in both cases of L-MFAP and H-MFAP. Due to these results, we focus only on the performance of the pico_UE in the three following case studies.

Firstly, by using (16), we evaluated the SINR of a pico_UE, by varying two parameters: the distance between the pico_UE and its serving cell ($D_p \in [5, 100]$ m), and the distance between the pico_UE and the L-MFAP ($d_{M\text{-}FAP} \in [2, 50]$ m). The simulation results reported in Fig. 7 show a very wide variation of SINRpico_UE values. More specifically, Fig. 8 shows the couple of values of D_p and $d_{M\text{-}FAP}$ when the SINR of the pico_UE reaches the minimum admissible value for each type of modulation, e.g. SINR $= \{-2.6, 10.9, 19.13\}$ dB (see Table 1). Let's note that in the region when the SINRpico_UE < -2.6 dB, the connections are dropped, in fact, in this case, the UE can't demodulate the signal in according to Table 1, and it may occur even in cases where the pico_UE is not so far away from serving picocell ($D_p > 10$ m).

In order to evaluate the total throughput of a picocell crossed by a bus equipped with a L-MFAP, we have considered a second urban setup. We perform a series of Matlab simulations in which there are N greedy pico_UEs randomly placed with a uniform distribution in a picocell area with a radius of 100 mt and a bus crosses the picocell with constant velocity v = 20 m/s and with a random distance from the pico base station. We assume that the

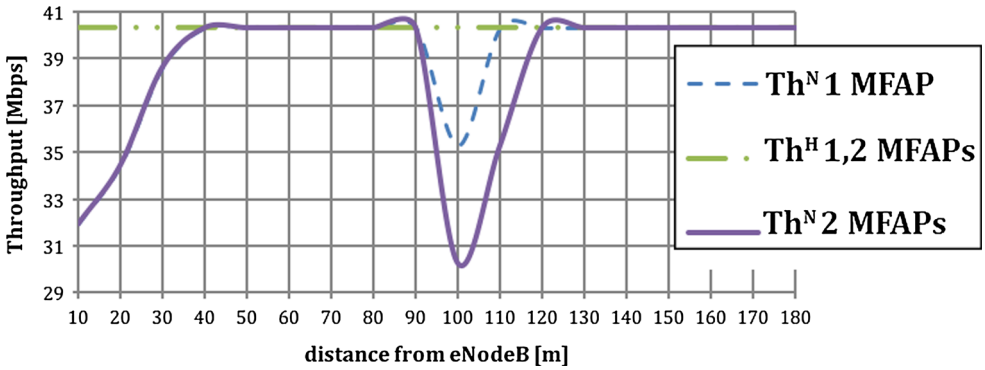

Fig. 5 System throughput with 1 or 2 MFAPs in a configuration with L-MFAP in non-orthogonal allocation scheme with a vehicle (*dashed line*) and two vehicles (*solid line*). The *line with dots* and *dashes* shows the system throughput in a scenario with 1 or 2 H-MFAPs

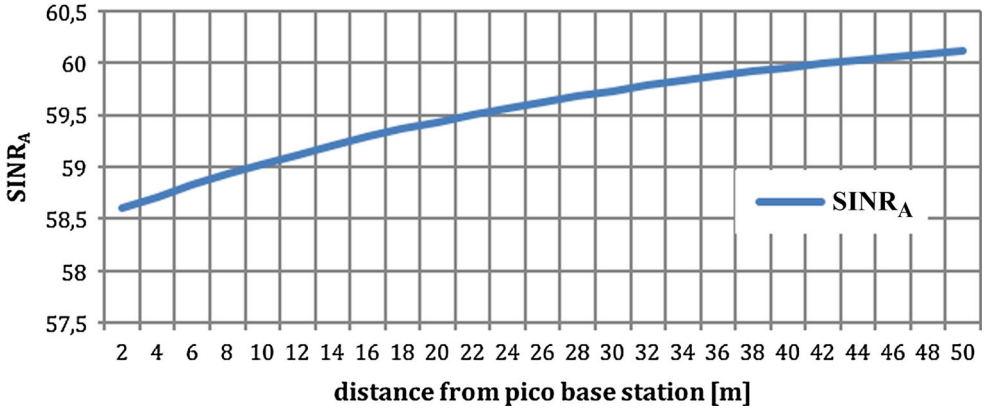

Fig. 6 $SINR_A$ measured by a VUE versus distance from the pico base station

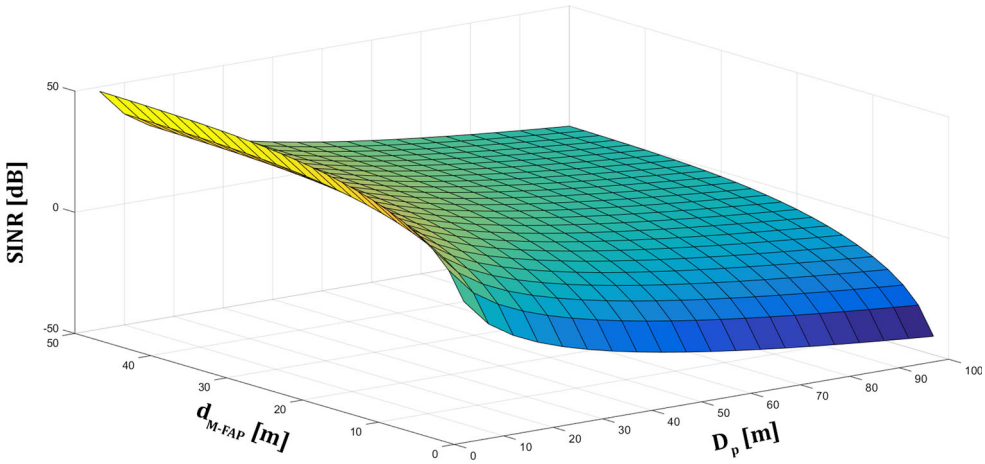

Fig. 7 $SINR_{pico\_UE}$ versus $d_{M\text{-}FAP}$ and D_p

resources are fairly allocated by the pico base station to the pico_UEs (N_{RB}/N Resource Blocks for each pico_UE). So, we calculate the instantaneous picocell as follows:

$$Th_{pico} = \sum_{i=1}^{N} \frac{N_{RB}}{N} * \frac{Q\left(SINR_{pico\_UE,i}\right)}{0.5 * 10^{-3}} \text{[bps]} \quad (28)$$

where $Q(SINR_{pico\_UE,i})$ is calculated by using (18) with the SINR measured using (16). Furthermore we compare this value with the one obtained in the same scenario but using a H-MFAP solution. Figure 9 shows the cdf of the average Th_{pico} values calculated with $N = 10$ greedy pico_UEs. We can see how the presence of the L-MFAP heavily degrades the throughput of the picocell.

For each simulation (same positions of the pico_UEs and same bus route), we also calculate the Throughput Gain with H-MFAP versus L-MFAP (see Fig. 10). The results demonstrate that the use of a H-MFAP makes the throughput of a picocell increased with an average of 24.88% with a standard deviation of 9.43%.

However, in Fig. 10 we can also note that the gain varies from about 5 to 50%. This is due to the random position of the bus respect the location of the pico base station. Based

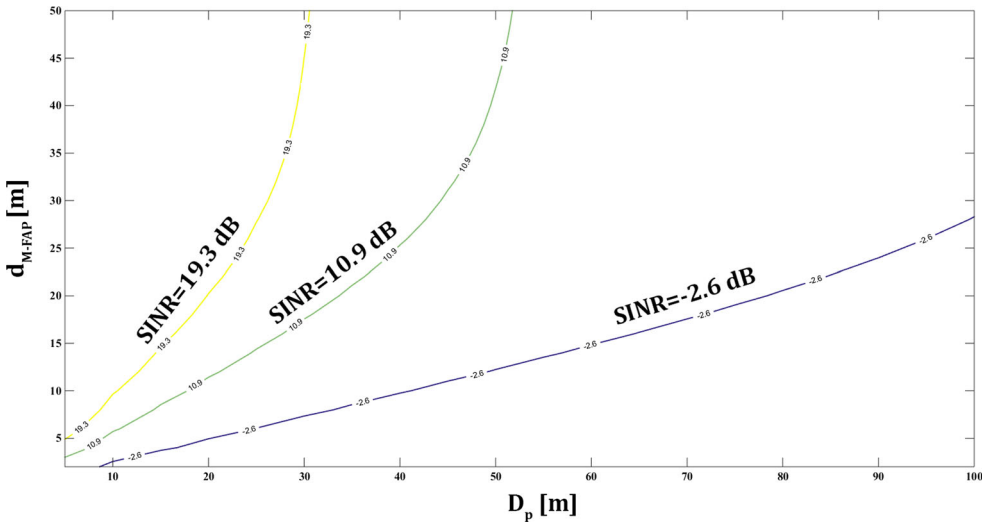

Fig. 8 Couple of values (D_p, $d_{M\text{-}FAP}$) for each SINR value considered

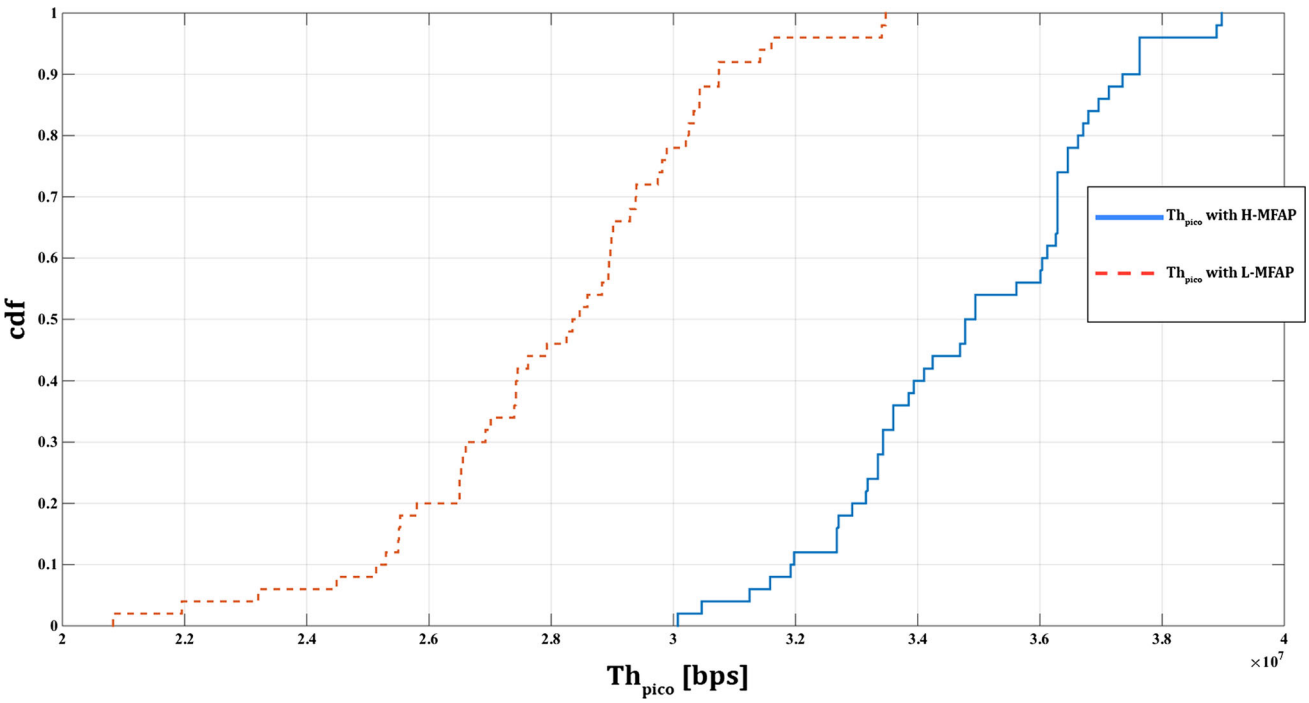

Fig. 9 Average picocell throughput (Th_{pico}) in bps for 10 pico_UE. The *solid line* is the Th_{pico} measured in a scenario with a H-MFAP. The *dotted line* is the Th_{pico} in the same scenario but with the presence of a vehicle equipped with a L-MFAP

on this observation, we wonder if in a realistic scenario will yet reached such a high gain value as to maintain high the throughput value. For this reason, in the following, we want to examine a third configuration, a typical urban setup proposed in Metis [53] and used by researchers in [5].

We simulate a simplified Madrid grid model with a heterogeneous deployment of macrocell, picocells, and L-MFAPs. In particular we consider a macro cell area with an eNodeB that transmits at 800 MHz where there are buildings of 120 by 120 m surrounded by streets of 21 m. The coverage of the streets is enhanced by the presence of LTE picocells, deployed as shown in Fig. 11. Both picocells and L-MFAPs work in the same LTE bandwidth, so there will be an interference between the transmissions of these two kinds of small cells.

We analyse a focus of the model by considering a group of 10 pico_UEs deployed along a street covered by the picocell. The positions of the pico_UEs are random with an uniform distribution. A bus equipped with L-MFAP across the street with a random route. Due to the small width of the streets, the density of the pico_UEs is higher and the L-MFAP is closer to them than the second configuration of

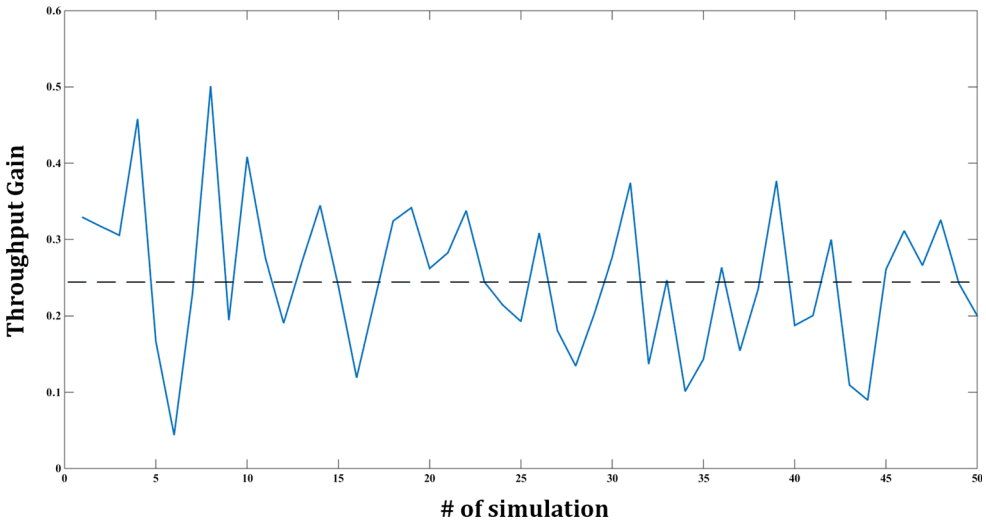

Fig. 10 Throughput gain value (*solid line*) measured in a single simulation, throughput gain (*dashed line*) averaged on 50 simulations

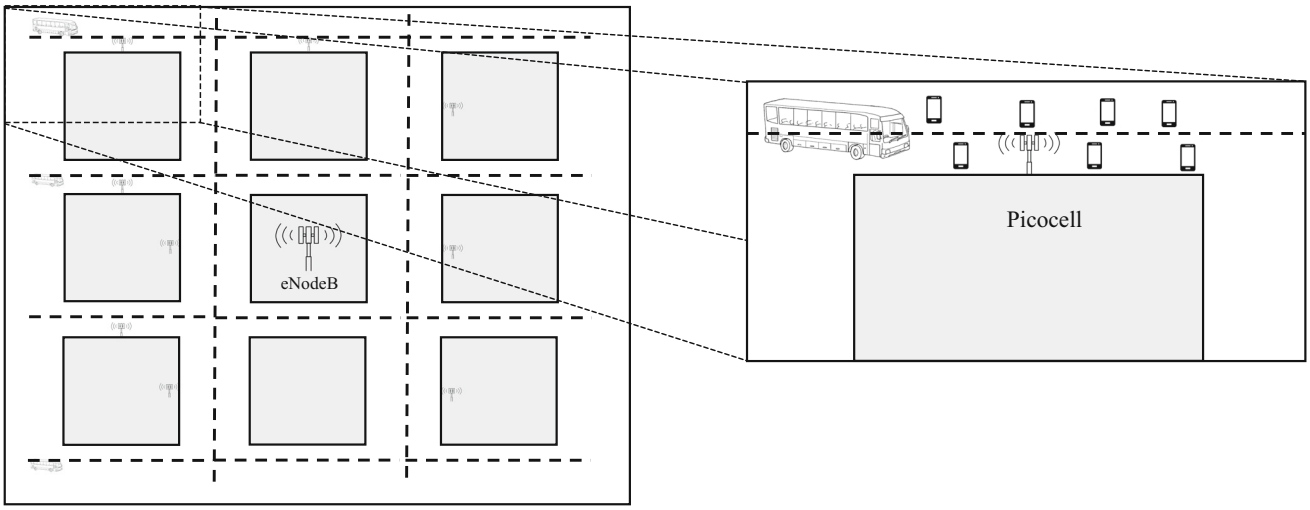

Fig. 11 Focus of Madrid grid model with a heterogeneous deployment of macrocell, picocells and vehicles equipped with MFAP

Scenario "Urban". We perform a series of simulations by varying the positions of the pico_UEs and the busses. For each simulation we collect the throughput of the picocell by using (28), and, with the same conditions, we replaced the L-MFAP with H-FAP. Finally, we calculate the cdf of the total average throughput of the picocell. The results are shown in Fig. 12. As in the second configuration of Scenario "Urban", the use of the H-MFAP in the bus increases the performance of the system. We calculated a Throughput Gain of 38.96% with a standard deviation of 7.84%.

8 Conclusion

In this paper we have introduced the concept of Hybrid-Mobile Femtocell, combining LTE and mmWave technologies, as a new proposal for the Moving Networks.

We have shown that the mmWave is a ready and suited technology to be applied in vehicular environments, so we analysed the feasibility of our proposal in two different system configuration that can be adopted in sub-urban and urban scenarios. In the first, L-MFAPs and eNodeB use the same frequency band, while in the latter, we consider that macrocells and small cells work in different LTE frequencies in order to eliminate the cross-layer interference. In particular we propose a scenario where eNodeB transmits at 800 MHZ, while both picocells and L-MFAP work at 2.6 GHz.

In order to compare H-MFAP performance with other pure L-MFAP solutions presented in literature, we have introduced a new throughput analysis, assuming the presence of greedy users and a fair allocation of RB to them. The simulation results in a "sub-urban" scenario show that the L-MFAP with orthogonal resource allocation

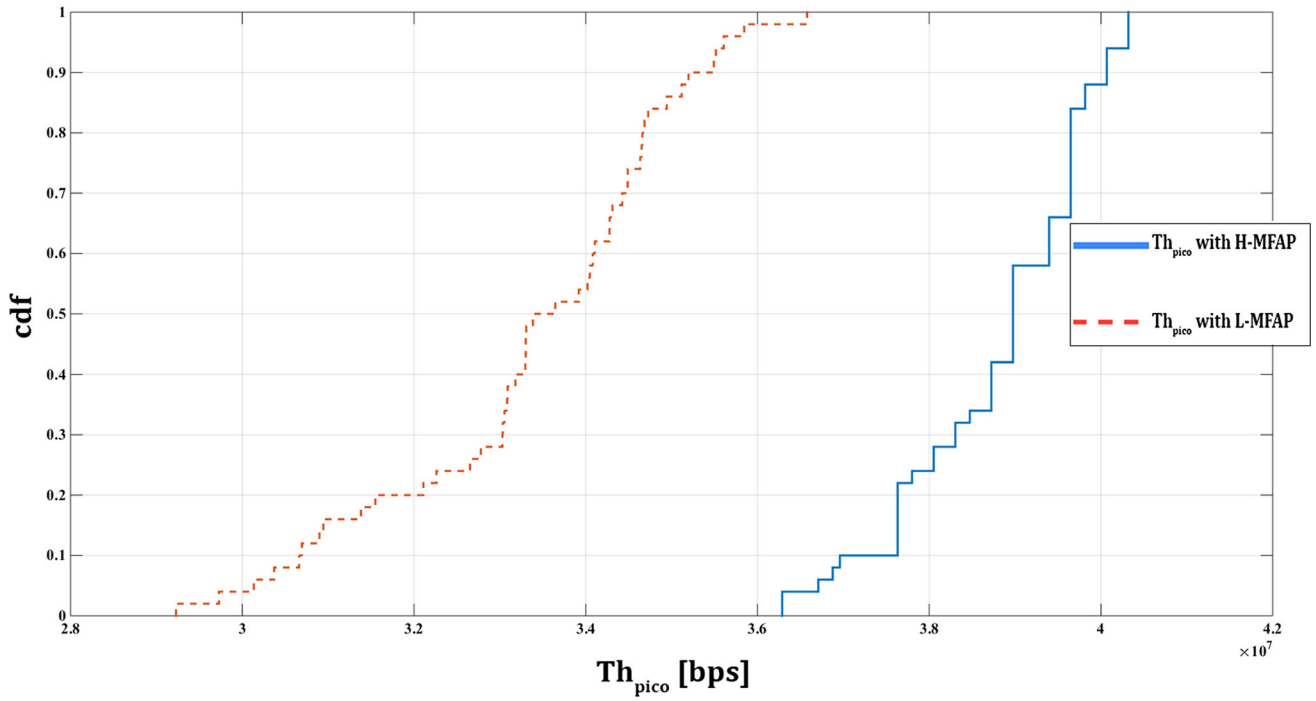

Fig. 12 Cdf of Th_{pico} in bps. The *solid line* is the Th_{pico} measured in a scenario with a bus with a H-MFAP. The *dotted line* is the Th_{pico} in the same scenario with the presence of a vehicle equipped with a L-MFAP

scheme always guarantees a constant throughput to the VUEs, but with a waste of 25% of the resources with a single vehicle. The L-MFAP with non-orthogonal scheme, instead, achieves higher performance compared to that with the orthogonal scheme, but it suffers from the interference due to simultaneous transmission of the direct and access links. In particular we have noted the throughput of the VUE decreases when the bus is close to the eNodeB and the out_UE suffers from the presence of the L-MFAP when it is closed to him.

We have also evaluated when there are two neighbouring vehicles equipped with MFAP. It has not been measured a significant inter-MFAP interference that can alter the throughput for the VUEs in both scenarios with two L-MFAP and two H-MFAP thanks to the double insulating effect of the VPL. However, the proximity of two L-MFAPs with non-orthogonal allocation scheme greatly worsens the throughput of the out_UE, while the performance of this user remain unchanged when one or more H-MFAPs are near to it. This is an important result that provides the characteristics of scalability and robustness to our proposal.

So, in a "sub-urban" scenario, our proposal outperforms L-MFAP with both allocation schemes. In fact, the H-MFAP always presents an increase in overall throughput of 33% compared to the L-MFAP operating in orthogonal allocation mode, and it does not suffer from the drastic reduction in throughput that L-MAF with non-orthogonal allocation scheme exhibits when the vehicle is close to the eNodeB and/or an out_UE.

We have extended our analysis in an "Urban" topology where different kind of small cells can be deployed. In this case, we have analysed the performance of the pico_UEs connected to a picocell that transmits in the same LTE band of the L-MFAP. Once again, in several case studies, the L-MFAP with non-orthogonal allocation scheme heavily decreases the throughput of the pico_UEs located along its route. For example, we have evaluated that in a simplified Madrid grid model, the use of H-MFAP improves the performance of the pico_UEs, obtaining a gain of about 39% than the solution with L-MFAP as suggested in literature.

In conclusion, in both sub-urban and urban deployment, the use of H-MFAPs guarantees high throughput to vehicular, macro, and pico users in any position where a vehicle can be, without excessive handover procedures and without waste of resources. So, we believe that H-MFAP can be a potential candidate for the Moving Network in 5G era.

Acknowledgements Funding was provided by Ministero dell'Istruzione, dell'Università e della Ricerca (Grant No. PON 03PE_00132_1 "Servify").

References

1. Hwang, I., Song, B., & Soliman, S. S. (2013). A holistic view on hyper-dense heterogeneous and small cell networks. *IEEE*

Communications Magazine, 51(6), 20–27. doi:10.1109/MCOM.2013.6525591.
2. Nokia siemens networks. (2011). 2020: beyond 4G radio evolution for the gigabit experience, white paper.
3. Cisco Visual Networking Index. (2016). Global mobile data traffic forecast update, 2015–2020, white paper.
4. Qualcomm Incorporated. (2013). The 1000× data challenge. http://www.qualcomm.com/1000x/.
5. Sui, Y., Guvenc, I., & Svensson, T. (2015). Interference management for moving networks in ultra-dense urban scenarios. *EURASIP Journal on Wireless Communications and Networking, 1,* 1–32. **(Springer International Publishing)**.
6. Osseiran, A., et al. (2014). Scenarios for the 5G mobile and wireless communications: the vision of the METIS project. *IEEE Communications Magazine, 52*, 26–35.
7. Ericsson. (2011). More than 50 billion connected devices, white paper.
8. Bogale, T. E., & Le, L. B. (2015). Massive MIMO and Millimeter Wave for 5G Wireless HetNet: Potentials and challenges. CoRR, vol. abs/1510.06359.
9. Huawei. (2014). 5G: A technology vision, white paper.
10. Wang, C.-X., et al. (2014). Cellular architecture and key technologies for 5G wireless communication networks. *IEEE Communications Magazine, 52*(2), 122–130.
11. Jangsher, S., & Li, V. O. K. (2013). Resource allocation in cellular networks employing mobile femtocells with deterministic mobility. In *Wireless Communications and Networking Conference (WCNC), 2013 IEEE* (pp. 819–824), 7–10 April.
12. Tanghe, E., Joseph, W., Verloock, L., & Martens, L. (2008). Evaluation of vehicle penetration loss at wireless communication frequencies. *IEEE Transactions on Vehicular Technology, 57*(4), 2036–2041.
13. Andrews, J. G., Claussen, H., Dohler, M., Rangan, S., & Reed, M. C. (2012). Femtocells: Past, present, and future. *IEEE Journal on Selected Areas in Communications, 30*(3), 497–508. doi:10.1109/JSAC.2012.120401.
14. Dudnikova, A., Panno, D., & Mastrosimone, A. (2015). Measurement-based coverage function for green femtocell networks. *Computer Networks, 83*, 45–58. doi: 10.1016/j.comnet.2015.02.025. ISSN 1389-1286.
15. Chandrasekhar, V., Andrews, J., & Gatherer, A. (2008). Femtocell networks: A Survey. *IEEE Communication Magazine, 46*(9), 59–67.
16. Haider, F., Wang, C., Haas, H., Yuan, D., Wang, H., & Gao, X., et al. (2011). Spectral efficiency analysis of mobile femtocell based cellular systems. In *IEEE 13th International Conference on Communication Technology*.
17. Chen, Y., & Lagrange, X. (2014). Downlink capacity gain analysis of mobile relay in LTE-Advanced network. In *Consumer Communications and Networking Conference (CCNC), 2014 IEEE 11th* (pp. 544–550), 10–13 January.
18. Chowdhury, M. Z., Lee, S. Q., Ru, B. H., Park, N., & Jang, Y. M. (2011). Service quality improvement of mobile users in vehicular environment by mobile femtocell network deployment. In *International Conference on ICT Convergence (ICTC), 2011* (pp. 194–198), 28–30 September.
19. Sui, Y., Vihriala, J., Papadogiannis, A., Sternad, M., Yang, W., & Svensson, T. (2013). Moving cells: A promising solution to boost performance for vehicular users. *IEEE Communications Magazine, 51*(6), 62–68.
20. Mastrosimone, A., & Panno, D. (2015). New challenge: moving network based on mmWave technology for 5G era. In *International Conference on Computer, Information and Telecommunication Systems 2015*. Gijon, Spain.
21. Mastrosimone, A., & Panno, D. (2015). A comparative analysis of mmWave vs LTE technology for 5G moving networks. In *The 11th IEEE International Conference on Wireless and Mobile Computing, Networking and Communications (WiMob 2015)*. Abu Dhabi, UAE.
22. Dehos, C., Gonzàles, J. L., De Domenico, A., Kténas, D., & Dussopt, L. (2014). Millimeter-Wave access and backhauling: The solution to the exponential data traffic increase in 5G Mobile Communications System? *IEEE Communications Magazine, 52,* 88–95.
23. Pi, Z., & Khan, F. (2011). An introduction to Millimeter-wave mobile broadband systems. *IEEE Communications Magazine, 49*(6), 101–107. doi:10.1109/MCOM.2011.5783993.
24. Hailan, P., Yamamoto, T., & Suegara, Y. (2015). LTE/WiGig RAN-level interworking architecture for 5G millimeter-wave heterogeneous networks. *IEICE Transactions on Communications, 98*(10), 1957–1968.
25. Damnjanovic, A., Montojo, J., Wei, Y., Ji, T., Luo, T., Vajapeyam, M., et al. (2011). A survey on 3GPP heterogeneous networks. *IEEE Wireless Communications, 18*(3), 10–21. doi:10.1109/MWC.2011.5876496.
26. GPP TR 36.836 Technical Specification Group Radio Access Network; Evolved Universal Terrestrial Radio Access (E-UTRA); Study on mobile relay (June 2014) by 3rd Generation Partnership Project.
27. Li, W., Zhang, C., Duan, X., Jia, S., Liu, Y., & Zhang, L. (2012). Performance evaluation and analysis on group mobility of mobile relay for LTE advanced system. In *Vehicular Technology Conference (VTC Fall), 2012 IEEE* (pp. 1–5), 3–6 September. doi: 10.1109/VTCFall.2012.6399277.
28. Raheem, R., Lasebae, A., Aiash, M., & Loo, J. (2013). From fixed to mobile femtocells in LTE systems: Issues and challenges. In *Second International Conference on Future Generation Communication Technology (FGCT), 2013* (pp. 207–212), 12–14 November. doi: 10.1109/FGCT.2013.6767218.
29. Chae, S., Nguyen, T., & Jang, Y. M. (2013). A novel handover scheme in moving vehicular femtocell networks. In *Fifth International Conference on Ubiquitous and Future Networks (ICUFN), 2013* (pp. 144–148), 2–5 July. doi: 10.1109/ICUFN.2013.6614800.
30. Chowdhury, M. Z., Chae, S. H., & Jang, Y. M. (2012). Group handover management in mobile femtocellular network deployment. In *Fourth International Conference on Ubiquitous and Future Networks (ICUFN), 2012* (pp. 162–165), 4–6 July. doi: 10.1109/ICUFN.2012.6261685.
31. Raheem, R., Lasebae, A., & Loo, J. (2014). Performance evaluation of LTE network via using Fixed/Mobile Femtocells. In *28th International Conference on Advanced Information Networking and Applications Workshops*.
32. Haider, F., Dianati, M., & Tafazolli, R. (2011). A simulation based study of mobile femtocell assisted LTE networks. In *7th International Wireless Communication and Mobile Computing Conference (IWCMC), 2011* (pp. 2198–2203), 4–8 July.
33. IEEE 802.15.3c Part 15.3: Wireless medium access control (MAC) and physical layer (PHY) specifications for high rate wireless personal area networks (WPANs) amendment 2: Millimeter-wave-based alternative physical layer extension, October 2009.
34. IEEE 802.11ad. Part 11: Wireless LAN medium access control (MAC) and physical layer (PHY) specifications—amendment 3: Enhancements for very high throughput in the 60 GHz band, December 2012.
35. Shokri-Ghadikolaei, H., Fischione, C., Fodor, G., Popovski, P., & Zorzi, M. (2015). Millimeter wave cellular networks: A MAC layer perspective. *IEEE Transactions on Communications, 63*(10), 3437–3458. doi:10.1109/TCOMM.2015.2456093.
36. Dahlman, E., et al. (2014). 5G radio access. *Ericsson Review, 91*(1), 42–47.

37. Okasaka, S., et al. (2016). Proof-of-concept of a Millimeter-Wave integrated heterogeneous network for 5G cellular. *Sensors, 16,* 1362. doi:10.3390/s16091362.
38. Weiler, R., et al. (2014). Enabling 5G backhaul and access with Millimeter-waves. In *Proceedings of the EuCNC*.
39. Collotta, M., & Pau, G. (2017). An innovative approach for forecasting of energy requirements to improve a smart home management system based on BLE. *IEEE Transactions on Green Communications and Networking*. doi:10.1109/TGCN.2017.2671407.
40. Costa, D. G., Collotta, M., Pau, G., & Duran-Faundez, C. (2017). A fuzzy-based approach for sensing, coding and transmission configuration of visual sensors in smart city applications. *Sensors, 17,* 93. doi:10.3390/s17010093.
41. Peraso. Perasotechcom. (2017). http://www.perasotech.com/. Accessed January 18, 2017.
42. SiBEAM—Home. Sibeamcom. (2017). http://www.sibeam.com. Accessed January 18, 2017.
43. Infineon. (2017). http://www.infineon.com/cms/en/product/rf-and-wireless-control/mm-wave-mmic/mmw-backhaul/BGT60/productType.html?productType=5546d46247342c630147918436016a3b. Accessed January 18, 2017.
44. Latticesemi. (2017). http://www.latticesemi.com/Products.aspx#_9ED6678E51A540A0BAB3EF178618CC4E. Accessed January 18, 2017.
45. Qualcomm. (2017). https://www.qualcomm.com/products/vive/11ad. Accessed January 18, 2017.
46. Analog. (2017). http://www.analog.com/en/products/rf-microwave/integrated-transceivers-transmitters-receivers/microwave-mmwave-tx-rx.html. Accessed January 18, 2017.
47. Collotta, M. (2015). FLBA: A fuzzy algorithm for load balancing in IEEE 802.11 networks. *Elsevier Journal of Network and Computer Applications, 53*, 183–192. doi: 10.1016/j.jnca.2015.04.005. ISSN: 10848045.
48. Huang, K.-C., & Wang, Z. (2011). *Millimeter Wave communication systems*. New York: Wiley-IEEE Press. ISBN 978-0-470-40462-1.
49. Bay, T., Alkhateeb, A., & Heat, R. W. (2014). Coverage and capacity of Millimeter-Wave cellular networks. *IEEE Communications Magazine, 52,* 70–77.
50. GPP, Technical Specification Group Radio Access Network; Evolved Universal Terrestrial Radio Access (E-UTRA); Further advancements for E-UTRA physical layer aspects (Rel. 9) TR 36.814 v.9.0.0, 3GPP, 2010.
51. Geng, S., Kivinen, J., Xiongwen, Z., & Vainikainen, P. (2009). Millimeter-Wave propagation channel characterization for short-range wireless communications. *IEEE Transactions on Vehicular Technology, 58*(1), 3–13.
52. Sesia, S., Baker, M., & Toufik, I. (2011). *LTE—the UMTS long term evolution: From theory to practise* (II ed.). New York: Wiley.
53. Agyapong, P., Braun, V., Fallgren, M., Gouraud, A., Hessler, M., Jeux, S., & Weber, A., et al. (2013). ICT-317669-METIS/D6.1 simulation guidelines. *Technical report*.
54. Willis, M. (2007). An introduction to radiowave propagation, course notes. Dr Mike Willis 2007. http://www.mike-willis.com/Tutorial/PF5.htm.
55. Hong, W., Baek, K., Kim, Y., Lee, Y., & Kim, B. (2014). mmWave phased-array with hemispheric coverage for 5th generation cellular handsets. In *8th European Conference on Antennas and Propagation (EuCAP), 2014* (pp. 714–716), 6–11 April. doi: 10.1109/EuCAP.2014.6901859.

Antonio Mastrosimone received his master's degree in Telecommunication Engineering with honors in October 2013 from the University of Catania where he is a Ph.D. Student of the Department of Electric, Electronic and Computer Science Engineering. His research focuses on 4G and 5G mobile networks, in particular on the applicability of heterogeneous wireless networks, the use of mmWave technology for vehicular environment.

Daniela Panno received the Dr. Ing. degree (with honors) in Electrical Engineering from the University of Catania, Italy, in 1989, and the Ph.D. degree in Electronic Engineering and Computer Science Engineering from the University of Palermo, Italy, in 1993. In 1989 she joined the Department of Computer Science and Telecommunications Engineering at the University of Catania, where she is now an Associate Professor of Telecommunications. She has attended several international workshops and symposia as invited speaker and she has served as Guest Editor for Computer Communications. Recent research interests include green networking, management and optimization of resources in ultra dense 5G networks, mobile services in IoT environment, routing algorithm in network on chip.